

ON THE ORIGIN OF INFRARED PLATEAU FEATURES IN PROTO-PLANETARY NEBULAE¹

SUN KWOK² AND KEVIN VOLK

Department of Physics and Astronomy, University of Calgary, 2500 University Drive, NW, Calgary, AL T2N 1N4, Canada;
kwok@iras.ucalgary.ca, volk@iras.ucalgary.ca

AND

PETER BERNATH

Department of Chemistry, University of Waterloo, Waterloo, ON N2L 3G1, Canada; bernath@uwaterloo.ca

Received 2001 January 11; accepted 2001 May 7; published 2001 May 23

ABSTRACT

The emission profiles of the 8 and 12 μm plateau features are derived from the *Infrared Space Observatory* spectra of proto-planetary nebulae. We suggest that these plateau features are primarily the result of alkane and alkene side groups on very large aromatic molecules and small carbonaceous particles. The relationship between the narrow aromatic hydrocarbon features and the 8 and 12 μm plateau features is discussed in a model of circumstellar chemical evolution where photochemical processing transforms the more aliphatic material in proto-planetary nebulae into more aromatic matter in planetary nebulae.

Subject headings: circumstellar matter — infrared: stars — ISM: lines and bands —
planetary nebulae: general — stars: AGB and post-AGB

1. INTRODUCTION

A family of strong infrared emission features at 3.3, 6.2, 7.7, 8.6, and 11.3 μm was first detected in the young carbon-rich planetary nebula (PN) NGC 7027 (Russell, Soifer, & Willner 1977). These features are now commonly found in the interstellar medium and have been identified as originating from various stretching and bending modes of aromatic hydrocarbon compounds (Duley & Williams 1981; Allamandola, Tielens, & Barker 1989). How and where these complex molecular materials form is an interesting problem of astrochemistry.

Since PNs evolve from asymptotic giant branch (AGB) stars, it would be useful to study the infrared spectra of the PN progenitors to search for the first appearance of these aromatic features. The infrared spectra of oxygen-rich AGB stars are dominated by the 10 and 18 μm silicate features, and approximately 4000 AGB stars have been observed by the *Infrared Astronomical Satellite (IRAS)* Low-Resolution Spectrometer (LRS) to show such features (Kwok, Volk, & Bidelman 1997). In carbon-rich AGB stars, the 11.3 μm SiC feature has been detected in over 700 stars. However, no AGB star is known to show the aromatic infrared bands (AIBs). It is therefore likely that the carriers of the AIB features are synthesized or excited after the termination of the AGB phase.

There is, however, evidence that the first step toward the synthesis of aromatic molecules occurs in the circumstellar envelopes of late AGB stars. The *Infrared Space Observatory (ISO)* has detected the vibrational bands of acetylene (C_2H_2) in a number of highly evolved carbon stars (Cernicharo et al. 1999; Volk, Xiong, & Kwok 2000). Because acetylene is a building block of benzene (Cherchneff, Barker, & Tielens 1992), its detection in carbon stars could be the first sign of the synthesis of aromatic molecules.

Observations of proto-planetary nebulae (PPNs), the short ($\sim 10^3$ yr) evolutionary phase between AGB stars and PNs, there-

fore holds the key to our understanding of the origin of the AIB. The discovery of large numbers of PPNs (see Kwok 1993) and the following ground-based (Geballe et al. 1992), *IRAS* (Jourdain de Muizon, d'Hendecourt, & Geballe 1990), and *ISO* (Hrivnak, Volk, & Kwok 2000) observations have shown that the AIB features are widely present in carbon-rich PPNs. However, the strengths of the AIB features in PPNs are different from those in PNs, and two features at 3.4 and 6.9 μm , identified as C–H aliphatic stretching and bending modes (Duley & Williams 1981; Joblin et al. 1996), are unique to PPNs (Kwok, Volk, & Hrivnak 1999). These spectral differences suggest that chemical evolution is still ongoing in the circumstellar envelope as the stars evolve from AGB stars to PNs.

Most interestingly, the infrared spectra of PPNs show strong, broad emission plateaus around 8 and 12 μm . These plateau features were first seen in the *IRAS* LRS (Kwok, Volk, & Hrivnak 1989) and Kuiper Airborne Observatory (Buss et al. 1990) spectra of PPNs. With higher sensitivity and improved spectral resolution, these plateau features are much better defined by *ISO* observations. In this Letter, we present an analysis of the 8 and 12 μm plateau features of PPNs and discuss their possible origins.

2. OBSERVATIONS

The observational results reported here are based on the *ISO* Short-Wavelength Spectrometer (SWS; de Graauw et al. 1996). The SWS observations were carried out in the SWS01 mode covering the spectral range 2.4–45 μm at speeds 1 or 2, giving effective resolutions of ~ 250 . The data were extracted from the *ISO* archive (from the following programs: IRAS Z02229+6208: bhrivnak.swsppn01; IRAS 16594–4656: pgarcia.pne; IRAS 22272+5435: proche.stardust; IRAS 19500–1709: bhrivnak.swsppn01; IRAS 23304+6147: bhrivnak.swsppn01).

The data reduction was carried out using version 7 of the standard pipeline processing. Once the autoanalysis results files had been obtained, they were further analyzed using the *ISO* Spectral Analysis Package. After obvious bad data points were removed, the data were averaged with a uniform wavelength spacing to produce the final spectra.

The SWS observations in bands 2A and 2B, from 4.08 to

¹ Based on observations made with the *Infrared Space Observatory*, an ESA project with instruments funded by the ESA member states (especially the PI countries: France, Germany, the Netherlands, and the UK) with the participation of ISAS and NASA.

² Canada Council Killam Fellow.

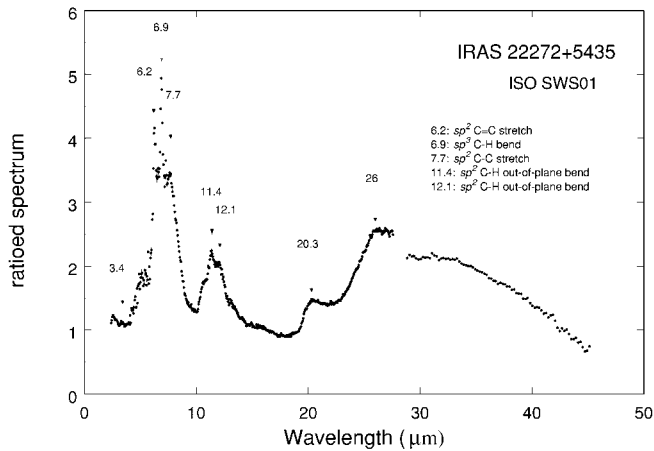


FIG. 1.—*ISO* SWS01 spectrum of IRAS 22272+5435 after the removal of a continuum. The detected narrow emission features and their peak wavelengths are marked on the spectrum. The identification of some of these features are listed in the legend.

7.00 μm , suffer from much worse signal-to-noise ratios (S/Ns) than the adjacent bands at longer and shorter wavelengths. This is primarily due to the noisier Si:Ga detectors used in SWS band 2 in the shorter wavelength sections as compared to the InSb detectors used in band 1 (2.38–4.08 μm). This is a general problem of all the SWS observations that we have reduced. The typical noise values in bands 2A and 2B are on the order of 6–10 times larger than those in band 1. In band 2C and band 3 the S/N value improves again because the PPNs are much brighter at wavelengths between 7 and 25 μm than they are at shorter wavelengths.

As an example of the plateau features, we show the *ISO* SWS01 spectrum of IRAS 22272+5435. This object was first discovered as a carbon-rich PPN from its infrared and optical properties (Kwok et al. 1989; Hrivnak & Kwok 1991). After the division of the spectrum by a dust continuum calculated with a radiation transfer model (Hrivnak et al. 2000), a number of broad and narrow features can be seen (Fig. 1). These include the AIB features at 6.2, 7.7, 11.3, and 12.2 μm , and the aliphatic C–H bend at 6.9 μm , as well as the well-known unidentified 20.1 μm (Volk et al. 1999) and 30 μm (Forrest, Houck, & McCarthy 1981) emission features. Two strong plateau features at 8 and 12 μm can also clearly be seen.

Similar continuum-divided spectra for IRAS Z02229+6208, 16594–4656, 19500–1709, and 23304+6147 are shown in Figure 2. In the case of 19500–1709, we have replaced the poor SWS band 2A and 2B data with the *ISO* spectrophotometer (PHT-S) data. It can be seen that the 8 μm plateau feature is strongest in 23304+6147, followed by 22272+5435 and 16495–4656. The features generally have similar shapes and peak wavelengths, with the exception of Z02229+6208, where the peak wavelength occurs at a shorter wavelength.

For the 12 μm plateau feature, it is strongest in 22272+5435, followed by 02229+6208 and 19500–1709. The 12 μm plateau feature is smoother than the 8 μm plateau feature, with the 11.3 and 12.2 μm features the only distinguishable narrow features.

3. EMISSION PROFILES OF THE PLATEAU FEATURES

With the spectral data for these PPNs, we are in position to derive the intrinsic emission profiles of the plateau features. First, we need to separate the contributions by the two pla-

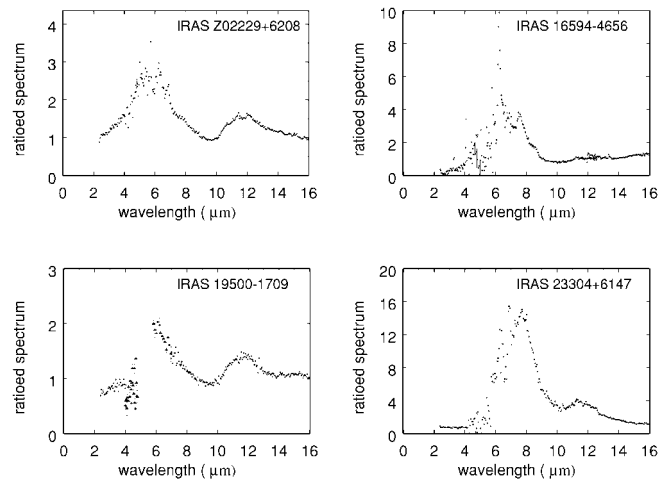


FIG. 2.—*ISO* SWS01 spectra of IRAS Z02229+6208, 16594–4656, 19500–1709, and 23304+6147 showing the 8 and 12 μm plateau features. A dust continuum has been divided out in each of the spectra. In the case of 19500–1709, the PHT-S data (*triangles*) are plotted instead of the SWS 2A and 2B band data.

teau features to the overall spectrum. For example, the long-wavelength side of the 8 μm feature appears to extend and overlap with the short-wavelength side of the 12 μm feature. In order to ensure that the continuum is completely removed, we first subtract a small linear baseline between 3.8 and 18 μm in the spectrum. We then eliminated the data from 9.4 to 16.4 μm where the overlap occurs. A polynomial was then fitted to the 8 μm feature from 7.9 μm onward, including the section from 16.4 to 19 μm . The plateau function has narrower features at 6.2, 6.9, 7.3, 7.7, and 8.2 μm . The last feature is quite weak.

The profile of the 12 μm plateau feature was found by subtracting the assumed polynomial shape of the 8 μm profile from the ratioed spectrum of 22272+5435. The resulting profile function has narrow peaks at 11.4, 12.1, 13.4, and 14.2 μm . The wings of the profile extend to 17.4 μm , after which the profile was cut off.

The resultant emission profiles are normalized to a maximum of 1 and plotted in Figure 3. The peaks of the profiles are at 6.8 and 11.4 μm , respectively. Other than the sharp emission

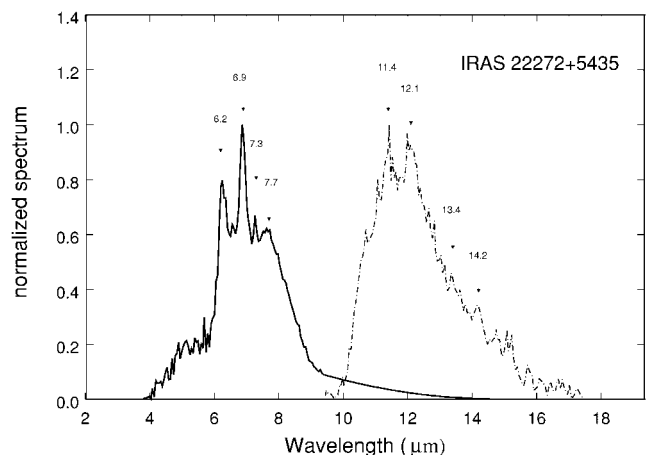


FIG. 3.—Normalized emission profiles of the 8 and 12 μm plateau of IRAS 22272+5435.

features (most of which can be identified), the underlying continuum is relatively smooth for both the 8 and 12 μm plateaus.

4. DISCUSSION

The detection of the strong infrared plateau features has raised questions about their relationship with the narrower AIB features. The fact that these plateau features are most prominent in the PPN phase suggests they represent a transient phenomenon lasting only about 10^3 yr. The previous detections of the 3.4 and 6.9 μm features in PPNs and their probable identification as arising from aliphatic bonds raises the question whether the plateau features could also originate from similar structures. The identification of the carrier of these plateaus is important, for they can provide clues about chemical evolution in the circumstellar environment.

4.1. The Origin of the 8 and 12 μm Plateaus

In the 8 μm region, the narrow features at 6.2, 7.7, and 8.6 μm can be identified as aromatic C=C and C–C stretches and the in-plane C–H bend, respectively. These narrow features sit on top of a broad plateau, which (as discussed below) can be attributed to alkyl bands and, to a lesser extent, alkene vibrations (Bellamy 1975). The strong band at 6.9 μm is clearly due to a mixture of $-\text{CH}_2-$ bend and $-\text{CH}_3$ antisymmetric bending modes (Bellamy 1975). This band is strong and characteristic of alkanes. As pointed out by Allamandola et al. (1989), there is also an aromatic ring mode of moderate intensity at 6.9 μm , but it is not a reliable aromatic marker because, to quote Bellamy, “This band is frequently overlaid by strong CH_2 deformations and its utility for identification purposes is therefore reduced ...”. In other words, the presence of strong 6.9 and 3.4 μm bands is characteristic of alkane side groups attached to aromatic rings.

Associated with the 6.9 μm $-\text{CH}_3$ band is a sharp symmetric $-\text{CH}_3$ bending mode at 7.25 μm and modes due to $-\text{C}(\text{CH}_3)_3$ (Fig. 4, site e) at 8.16 μm and $=\text{C}(\text{CH}_3)_2$ (Fig. 4, site f) at 8.6 μm (Bellamy 1975). Weaker in-plane C–H bending modes also contribute from 7.0 to 7.6 μm . When the $-\text{CH}_2-$ groups are in the form of cyclic rings—for example, in hydrogenated aromatic rings—they also give rise to a wide range of features in the 8 μm region. A force field calculation by Sehra & Duley (2000) has shown that hydrogenated aromatic rings have a “quasi-continuum between 6–9 μm .” We therefore assign the 8 μm plateau to a mixture of modes primarily associated with alkane side groups, with some alkenyl contributions, attached to aromatic rings.

The strong emission feature at 11.3 μm is commonly assigned to aromatic out-of-plane vibrations (Allamandola et al. 1989). A series of bands at about 12.1, 12.4, and 13.3 μm (Kwok et al. 1999; Hrivnak et al. 2000) have been attributed to aromatic out-of-plane C–H bands with two, three, and four adjacent hydrogens, respectively (Allamandola et al. 1989; Herlin et al. 1998). These features have been detected in the spectrum of the PPN IRAS 07134+1005 (Kwok et al. 1999). However, these AIB features should be accompanied by a complex set of features due to out-of-plane vibrations of alkenes (Bellamy 1975), resulting in a plateau feature about 10.5–13.3 μm (FWHM). It is therefore possible that the 12 μm plateau feature is associated with C–H out-of-plane bending modes for a wide variety of alkene ($-\text{CH}=\text{CHCH}_3$; Fig. 4, site a) and aromatic molecules (Bellamy 1975). These alkenes may be connected directly (Fig. 4, site a) or indirectly ($-\text{CH}_2\text{CH}=\text{CH}_2$; Fig. 4, site b) through an alkyl $(\text{CH}_2)_n$ linkage to aromatic rings but are not

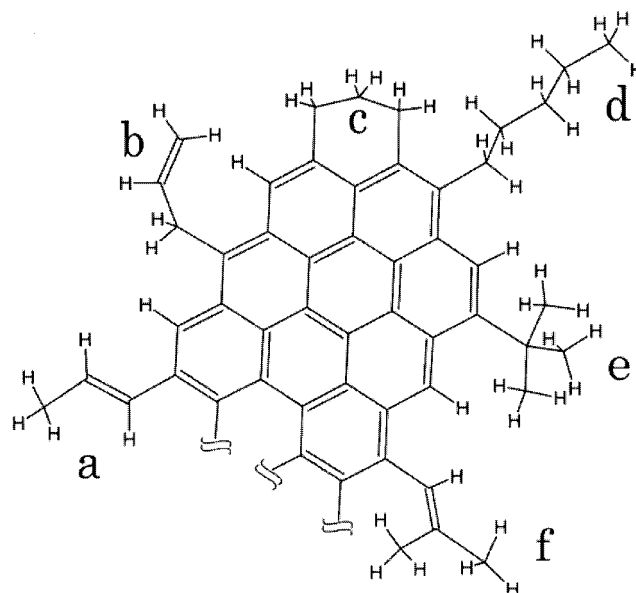


FIG. 4.—Schematic chemical diagram illustrating the various side groups attached to aromatic rings that contribute to the plateau emissions.

part of a ring system. Cyclic alkanes ($-\text{CH}_2\text{CH}_2\text{CH}_2-$; Fig. 4, site c) may also contribute in the short-wavelength part (9.5–11.5 μm) of this band, and long chains of four or more $-\text{CH}_2-$ groups [$-(\text{CH}_2)_4\text{CH}_3$; Fig. 4, site d] may contribute to the long-wavelength end (13.9 μm ; Bellamy 1975).

The fact that the 11.3 μm AIB feature is strong in PNs suggest that the aromatic content is much higher in PNs than PPNs (Guillois et al. 1996; Kwok et al. 1999). It is very likely that PPNs also contain substantial numbers of alkyl groups, but these groups do not have strong bands in the 12 μm region (with the exception of cyclic alkanes and long $-\text{CH}_2-$ groups mentioned above). The $-\text{CH}=\text{CH}_2$, $-\text{CH}=\text{CH}-$, $\text{C}=\text{CH}_2$, and $\text{C}=\text{C}-\text{H}$ groups all have out-of-plane bending modes in the 10–12.6 μm range. Although some of these modes are relatively sharp, the mixture of alkene, aromatic, and cyclic alkane groups will tend to wash this structure out. The 12 μm plateau is thus assigned to a mixture of out-of-plane C–H alkene modes, with some modest contributions from alkyl and aromatic groups.

The photochemistry of complex organic molecules has been studied extensively by physical organic chemists. When gas-phase alkanes absorb UV light, the primary photochemical event is the elimination of molecular hydrogen to form alkenes (Gilbert & Baggott 1991). Minor channels are the cleavage of C–H and C–C bonds to form free radicals. Alkenes, in contrast, have a much richer UV photochemistry. They undergo a variety of isomerizations, bond migrations, and cyclization reactions. Of particular interest are the ring closure reactions and cycloaddition reactions that transform alkenes into ring systems. Additional hydrogen loss can then result in fully aromatic rings that are more stable than alkanes or alkenes. The net result of UV irradiation is thus the transformation of aliphatic to aromatic groups. Similar transformations of hydrogenated amorphous carbon have also been discussed by Duley (2000). The evolution of PPNs to PNs is consistent with these chemical transformations.

In summary, we propose that the 8 and 12 μm plateau features in PPNs are due to the presence of a wide variety of alkane and alkene groups attached to hydrogenated aromatic

rings. As these compounds are irradiated with UV light as PPNs evolve to PNs, these aliphatic side groups are modified, leading to larger aromatic ring systems and stronger AIB features at the expense of the aliphatic and plateau features.

4.2. Gas or Solid?

Although the AIB features seen in the interstellar medium have been widely attributed to mixtures of gas-phase polycyclic aromatic hydrocarbon (PAH) molecules transiently heated by interstellar UV photons, this model is unlikely to apply to PPNs. The temperatures of the central stars of PPNs are too low to emit any significant number of UV photons, and the excitation of the AIB features has to rely on visible photons. Since neutral PAH molecules have small absorption cross sections in the visible, the carriers of the AIB bands in PPNs are more likely to be dark solid-state materials that absorb equally well in the visible and in the UV. While it is known that PAH cations or anions can absorb visible light (Halasinski et al. 2000), there is no good reason to believe that the PAH molecules should be in ionic form in the neutral environment of PPNs.

An alternative to the PAH hypothesis is bulk solid-state carbonaceous grains such as hydrogenated amorphous carbon (Jones, Duley, & Williams 1990), quenched carbonaceous composite (Sakata et al. 1987), or coal (Papoular, Reynaud, & Nenner 1991). The presence of various hydrogen-containing groups among the aromatic rings can lead to a rich emission spectrum in the infrared (Duley & Williams 1981). More specifically, the spectral change from PPNs to PNs has been compared to the progressive aromatization of coal (Guillois et al. 1996). It is interesting to note that semianthracite coal also

shows plateau features similar to those observed in PPNs. The coal model also has the advantage that the grain material provides for the underlying continuum, and a second carrier (e.g., amorphous carbon) therefore becomes unnecessary. Note that if very large PAH molecules are considered, then the distinction between gas and solid phase is not very meaningful. Clearly, the size distribution of large molecules overlaps with small solid grains.

5. CONCLUSIONS

The detection of the 3.4 and 6.9 μm features in PPNs suggests that these objects are rich in aliphatic compounds. From the *ISO* spectra of PPNs, we derived the emission profiles of these two plateau features and suggested that they arise from various bending modes of aliphatic side groups attached to aromatic rings. We identified the plateau features as arising from a complex collection of alkane and alkene side chains. As the result of UV processing, these side groups are destroyed in the PN phase, resulting in larger aromatic units and sharper AIB emission features. From the observed spectral changes between PPN and PN phases, we conclude that photochemistry is active in PN evolution.

We thank K. Tereszchuk for preparing Figure 4. This work is supported by grants to S. K., K. V., and P. B. from the Natural Science and Engineering Research Council of Canada. S. K. acknowledges the award of a Killam Fellowship from the Canada Council for the Arts. Partial support of this work was also provided by the Petroleum Research Fund of the American Chemical Society.

REFERENCES

- Allamandola, L. J., Tielens, A. G. G. M., & Barker, J. R. 1989, *ApJS*, 71, 733
 Bellamy, L. J. 1975, *The Infrared Spectra of Complex Molecules* (London: Chapman & Hall)
 Buss, R. H., Cohen, M., Tielens, A. G. G. M., Werner, M. W., Bregman, J. D., Rank, D., Witteborn, F. C., & Sandford, S. 1990, *ApJ*, 365, L23
 Cernicharo, J., et al. 1999, *ApJ*, 526, L41
 Cherchneff, I., Barker, J. R., & Tielens, A. G. G. M. 1992, *ApJ*, 401, 269
 de Graauw, T., et al. 1996, *A&A*, 315, L49
 Duley, W. W. 2000, *ApJ*, 528, 841
 Duley, W. W., & Williams, D. A. 1981, *MNRAS*, 196, 269
 Forrest, W. J., Houck, J. R., & McCarthy, J. F. 1981, *ApJ*, 248, 195
 Geballe, T. R., Tielens, A. G. G. M., Kwok, S., & Hrivnak, B. J. 1992, *ApJ*, 387, L89
 Gilbert, A., & Baggott, J. 1991, *Essentials of Molecular Photochemistry* (Oxford: Blackwell Scientific)
 Guillois, O., Nenner, I., Papoular, R., & Reynaud, C. 1996, *ApJ*, 464, 810
 Halasinski, T. M., Hudgins, D. M., Salama, F., Allamandola, L. J., & Bally, T. 2000, *J. Phys. Chem. A*, 104, 7484
 Herlin, N., Bohn, I., Reynaud, C., Cauchetier, M., Galvez, A., & Rouzaud, J.-N. 1998, *A&A*, 330, 1127
 Hrivnak, B. J., & Kwok, S. 1991, *ApJ*, 371, 631
 Hrivnak, B. J., Volk, K., & Kwok, S. 2000, *ApJ*, 535, 275
 Joblin, C., Tielens, A. G. G. M., Allamandola, L. J., & Geballe, T. R. 1996, *ApJ*, 458, 610
 Jones, A. P., Duley, W. W., & Williams, D. A. 1990, *QJRAS*, 31, 567
 Jourdain de Muizon, M., d'Hendecourt, L. B., & Geballe, T. R. 1990, *A&A*, 227, 526
 Kwok, S. 1993, *ARA&A*, 31, 63
 Kwok, S., Volk, K., & Bidelman, W. P. 1997, *ApJS*, 112, 557
 Kwok, S., Volk, K. M., & Hrivnak, B. J. 1989, *ApJ*, 345, L51
 ———. 1999, *A&A*, 350, L35
 Papoular, R., Reynaud, C., & Nenner, I. 1991, *A&A*, 247, 215
 Russell, R. W., Soifer, B. T., & Willner, S. P. 1977, *ApJ*, 217, L149
 Sakata, A., Wada, S., Onaka, T., & Tokunaga, A. T. 1987, *ApJ*, 320, L63
 Seahra, S. S., & Duley, W. W. 2000, *ApJ*, 542, 898
 Volk, K., Kwok, S., & Hrivnak, B. J. 1999, *ApJ*, 516, L99
 Volk, K., Xiong, G. Z., & Kwok, S. 2000, *ApJ*, 530, 408